Draft version January 4, 2017
Preprint typeset using LaTeX style emulateapj v. 08/22/09

arXiv:1602.00465v3 [astro-ph.GA] 3 Jan 2017

WHERE ARE THE LOW-MASS POPULATION III STARS ?

Tomoaki Ishiyama[1], Kae Sudo[2], Shingo Yokoi[2], Kenji Hasegawa[3], Nozomu Tominaga[2,4], and Hajime Susa[2]
Institute of Management and Information Technologies, Chiba University, 1-33, Yayoi-cho, Inage-ku, Chiba, 263-8522, Japan[1]
Department of Physics, Konan University, Okamoto, Kobe, Japan[2]
Graduate School of Science, Nagoya University, Furo-cho, Chikusa-ku, Nagoya, Aichi 464-8602, Japan[3] and
Kavli Institute for the Physics and Mathematics of the Universe (WPI),
The University of Tokyo, 5-1-5 Kashiwanoha, Kashiwa, Chiba 277-8583, Japan[4]
Draft version January 4, 2017

ABSTRACT

We study the number and the distribution of low mass Pop III stars in the Milky Way. In our numerical model, hierarchical formation of dark matter minihalos and Milky Way sized halos are followed by a high resolution cosmological simulation. We model the Pop III formation in H_2 cooling minihalos without metal under UV radiation of the Lyman-Werner bands. Assuming a Kroupa IMF from 0.15 to 1.0 $M_\odot$ for low mass Pop III stars, as a working hypothesis, we try to constrain the theoretical models in reverse by current and future observations. We find that the survivors tend to concentrate on the center of halo and subhalos. We also evaluate the observability of Pop III survivors in the Milky Way and dwarf galaxies, and constraints on the number of Pop III survivors per minihalo. The higher latitude fields require lower sample sizes because of the high number density of stars in the galactic disk, the required sample sizes are comparable in the high and middle latitude fields by photometrically selecting low metallicity stars with optimized narrow band filters, and the required number of dwarf galaxies to find one Pop III survivor is less than ten at < 100 kpc for the tip of red giant stars. Provided that available observations have not detected any survivors, the formation models of low mass Pop III stars with more than ten stars per minihalo are already excluded. Furthermore, we discuss the way to constrain the IMF of Pop III star at a high mass range of $\gtrsim 10 M_\odot$.

Subject headings: methods: numerical —early Universe —first stars —stars: low-mass —Galaxy: structure —dark matter

1. INTRODUCTION

First stars are born in the minihalos of $\sim 10^5 - 10^6 M_\odot$ approximately one hundred million years after the big bang (Haiman et al. 1996; Tegmark et al. 1997; Nishi & Susa 1999; Fuller & Couchman 2000; Abel et al. 2002; Bromm et al. 2002; Yoshida et al. 2003). In such environments, the H_2 molecule is the only coolant of the gas different from the nearby interstellar medium (ISM) which contains metals and dust grains. The mass of the first stars are expected to be more massive than their present-day counterparts because of the inefficient cooling via H_2. In fact, detailed studies, including cosmological radiation hydrodynamical simulations have shown that the first stars are very massive as a first approximation (Omukai & Nishi 1998; Omukai & Palla 2001, 2003; Bromm & Larson 2004; Yoshida et al. 2006, 2008; Hosokawa et al. 2011; Hirano et al. 2014, 2015).

However, the inefficiency of the cooling is also conducive to the formation of heavy circumstellar disks which are gravitationally unstable. The unstable disks fragment into small pieces, which could end up as low mass stars (Clark et al. 2008; Smith et al. 2011; Clark et al. 2011a,b; Greif et al. 2011a, 2012; Machida & Doi 2013; Susa 2013; Susa et al. 2014). If those low mass stars are less massive than $0.8 M_\odot$, their life times are longer than the age of the universe, and thus they could survive to be found in the present-day universe. However, the fates of the fragments are still uncertain theoretically. On the one hand, they could fall onto the central protostar and merge with it because of the efficient transportation of angular momentum in the disk (e.g., Vorobyov & Basu 2015; Hosokawa et al. 2015; Sakurai et al. 2016), but at the same time they could be ejected from the central dense region to highly eccentric orbits via many body gravitational interactions (e.g., Susa et al. 2014). In the former case, they cannot be the low mass stars, but in the latter case, the fragments could be long-lived low mass stars because of the poor mass accretion rate in such orbits.

Hence, the fraction of the fragments that survives as low mass stars and thus the average number of such low mass stars per minihalo is highly controversial, and it remains an open question.

The most straightforward way to approach this issue is to search the metal free stars in the Milky Way. In fact, there is a long history of the hunting for those stars (Beers & Christlieb 2005, and the references are therein). Recent surveys search the metal poor stars among $10^5 - 10^6$ stars (e.g. Keller et al. 2007; Yanny et al. 2009; Li et al. 2015), and many iron poor stars are found to be carbon enhanced metal poor stars (CEMPs). Some stars such as SDSS J102915+172927 (Caffau et al. 2011) are totally deficient in metals including carbon. However, no metal free star has been discovered so far.

The current state of observations of first star hunting implies that the surviving first stars are pretty rare in the Milky Way even if they exist. However, this fact

Electronic address: ishiyama@chiba-u.jp

only reveals that they are rare compared to other normal stars formed in the later different environments. We need to predict theoretically how many first stars should be found in the Milky Way assuming a certain model of star formation, or initial mass function (IMF) of those stars, in order to constrain the theory by the observations. At the same time, it is helpful to suggest the area in the sky where we should survey to find low mass first stars.

Several theoretical studies have been conducted to investigate this issue. Diemand et al. (2005) discussed whether stars should have a centrally condensed distribution in our Galactic halo than the dark matter mass distribution by analyzing the density peaks in their N-body simulations. On the other hand, Scannapieco et al. (2006) also tried to address the issue by focusing on the position of the metal free stars born in rather massive halos with virial temperatures of $T_{\rm vir} \gtrsim 10^4$K. They found that these stars should be distributed more smoothly in our Galactic halo, probably because these massive halos collapse at later epochs than the minihalos of $\sim 10^6 M_\odot$. Tumlinson (2010) investigated the spatial distribution of metal poor stars in the Milky Way, utilizing massive cosmological N-body simulation, and they found that the metal poor stars would be better found in the direction of the Galactic bulge. However, the mass resolutions of the N-body simulations used in these works were not enough to capture the formation of the minihalos of $\sim 10^6 M_\odot$.

Recently, Hartwig et al. (2015) discussed this issue by semi-analytic methods, and they give the expected number of first stars in our Galactic halo. They report that unbiased survey of 4×10^6 halo stars could impose a rather stringent constraint on the low mass end of the IMF. However, the spatial distribution of such stars cannot be derived because of the nature of semi-analytic methods.

In this paper, we perform a huge cosmological N-body simulation that resolve the minihalos and contains a few Milky Way sized halos in the simulation box. Assuming the first star formation model in minihalos, we can trace the stars until present-day universe and can give predictions for the number, location, and the apparent magnitudes of such stars. Compared with the past/ongoing/planning surveys of metal poor stars, we try to constrain the theoretical IMF of the first stars at the low mass end.

In §2, we describe the numerical model of the cosmological simulation. The number and the distribution of surviving first stars in the Milky Way are shown in §3. In §4, we show the number of the observable first stars and the probability distribution of finding those stars on the celestial sphere, assuming a galactic model. Then we derive the current constraint on the Pop III star formation model. §5 is devoted to discussion and §6 to summary.

2. MODEL DESCRIPTION

Hierarchical formation of dark matter minihalos and Milky Way sized halos are followed by a high resolution cosmological simulation. The formation of Pop III stars is simply modeled on merger trees of dark matter halos.

2.1. *Cosmological Simulation*

The cosmological simulation consists of 2048^3 dark matter particles in a comoving box of $8\,h^{-1}$Mpc. The mass resolution is $5.13 \times 10^3\,h^{-1}M_\odot$ and the gravitational softening length is $120\,h^{-1}$pc, which enable us to handle minihalos with sufficient resolution. We generated the initial condition by a publicly available code, 2LPTic[1], using second-order Lagrangian perturbation theory (e.g., Crocce et al. 2006). We used the online version[2] of CAMB (Lewis et al. 2000) to calculate the transfer function. The cosmological parameters adopted are consistent with an observation of the cosmic microwave background obtained by the Planck satellite (Planck Collaboration et al. 2014), namely, $\Omega_0 = 0.31$, $\Omega_b = 0.048$, $\lambda_0 = 0.69$, $h = 0.68$, $n_s = 0.96$, and $\sigma_8 = 0.83$. The initial and final redshifts are 127 and 0.

For the time integration, we used a massively parallel TreePM code, GreeM (Ishiyama et al. 2009a; Ishiyama et al. 2012) with the Phantom-GRAPE software accelerator [3](Nitadori et al. 2006; Tanikawa et al. 2012, 2013), on Aterui supercomputer at Center for Computational Astrophysics, CfCA, of National Astronomical Observatory of Japan. The snapshots were stored at the redshifts so that the logarithmic interval $\Delta \log(1+z)$ is 0.01. We carefully checked that how this interval affects the quality of merger trees. The value adopted here yields well converged merger rates.

To identify halos, we used the Friends-of-Friends (FoF) algorithm (Davis et al. 1985) with a linking parameter of $b = 0.2$. The smallest halo consists of 32 particles, which set the minimum FoF halo mass to be $1.6 \times 10^5\,h^{-1}M_\odot$. We extracted merger trees by the algorithm described in Ishiyama et al. (2015).

2.2. *Model for the Formation of Pop III Stars*

In our Pop III star formation model, Pop III stars are assumed to form in minihalos where virial temperature $T_{\rm vir}$ exceeds a threshold $T_{\rm vir}^{\rm crit}$. In such halos, H_2 molecules form efficiently and the gas collapses to form stars via H_2 line cooling. We also put an upper bound of $T_{\rm vir}$ so that we exclude the atomic cooling halos. We set the upper bound to be 2000K in this work. We calculated $T_{\rm vir}$ of the minihalos using a function proposed by Kitayama et al. (2001),

$$T_{\rm vir} = 9.09 \times 10^3 \left(\frac{\mu}{0.59}\right) \left[\frac{M(z_{\rm c})}{10^9\,h^{-1}M_\odot}\right]^{2/3} \times \left[\frac{\Delta_{\rm c}(z_{\rm c})}{18\pi^2}\right]^{1/3} (1+z_{\rm c})\,{\rm K}, \quad (1)$$

where μ is the mean molecular weight in units of the proton mass, $M(z_{\rm c})$ is the minihalo mass at the collapse redshift $z_{\rm c}$, and $\Delta_{\rm c}(z_{\rm c})$ is the mean overdensity of collapsed halos. We set $\mu = 1.22$, and used the mean overdensity according to the spherical collapse model (Bryan & Norman 1998). Other values are directly derived from the simulation.

Once Pop III stars form, UV radiation in the Lyman-Werner (LW) bands from the stars causes photodissociations of H_2 molecules and suppresses Pop III star formation in relatively lower mass halos. We used the criterion

[1] http://cosmo.nyu.edu/roman/2LPT/
[2] http://lambda.gsfc.nasa.gov/toolbox/tb_camb_form.cfm
[3] http://code.google.com/p/phantom-grape/

of the virial temperature under the LW background proposed by Machacek et al. (2001),

$$\left(\frac{T_{\rm vir}^{\rm crit}}{1000{\rm K}}\right) = 0.36\left[F_{\rm LW}\,(\Omega_b h^2)^{-1}\left(\frac{1+z}{20}\right)^{3/2}\right]^{0.22} \quad (2)$$

,where $F_{\rm LW}$ is the LW flux in a unit of $10^{-21}\,{\rm ergs}^{-1}\,{\rm cm}^{-2}\,{\rm Hz}^{-1}$. We assume spatially uniform and time dependent LW flux,

$$F_{\rm LW} = 4\pi J_{\rm LW} = 1.26\times10^{1.8(-1-\tanh(0.1(z-40)))}, \quad (3)$$

which is a fitting function derived to reproduce cosmological reionization simulations (Ahn et al. 2012).

By tracking the merger tree in descending redshift, we listed halos with $T_{\rm vir}^{\rm crit} < T_{\rm vir} < 2000$K as minihalos where Pop III stars are assumed to be born with the formation redshift $z_{\rm c}$. If any progenitors in the main branch of a halo are already listed, the halo is excluded from the list. The main branch of a halo is extracted by connecting the most massive progenitor of the most massive progenitor. This procedure ensures that gas in Pop III star forming halos is metal free. We terminated the list up at $z = 10$, when the reionization is assumed to start, since the photoheating accompanied by the reionization shut down the star formation in such minihalos. The upper limit of the virial temperature criterion is insensitive to the total number of minihalos. When we change the upper limit to 8000K from 2000K, the number of minihalos increases in only $\sim 1\%$.

2.3. *Pop III Survivors in the Present Universe*

The IMF of Pop III stars is still unknown, although there are some theoretical implications (e.g., Greif et al. 2011a; Hirano et al. 2014; Susa et al. 2014; Hirano et al. 2015). As discussed in §1, the low mass end is particularly uncertain even in theoretical models. Hence, we simply assume that the number $n_{\rm pop3}$ of low-mass Pop III stars with a main-sequence mass of 0.15–1.0$M_\odot$ formed in a minihalo. Then we try to constrain the theoretical models in reverse.

We selected randomly $n_{\rm pop3}$ dark matter particles from each minihalo as tracers of the low mass Pop III survivors. The spatial positions of the tracers at $z = 0$ are assumed to be those of Pop III survivors. In this study, we use $n_{\rm pop3} = 1$ and 10. We adopt a Kroupa IMF (Kroupa 2001) for the low-mass Pop III stars and randomly set the mass of each Pop III star. Their magnitudes of various bands at $z = 0$ are calculated from their masses and ages using an isochrone model with $Z = 0$ for stars with $M > 0.7M_\odot$ and $Z = 0.0001$ for stars with $M < 0.7M_\odot$ (Girardi et al. 2000; Marigo et al. 2001).[4] Since the lifetime of stars with masses larger than $\sim 0.8M_\odot$ is shorter than the cosmic time, these stars cannot survive and the number of Pop III survivors stars per minihalo is $\sim 0.9\ n_{\rm pop3}$.

3. Pop III STARS IN OUR GALACTIC HALO

Figure 1 shows the number of Pop III survivors, $N_{\rm surv}$ in each halo at $z = 0$ as a function of the halo mass. The number of survivors is proportional to the halo mass and

[4] http://pleiadi.pd.astro.it/

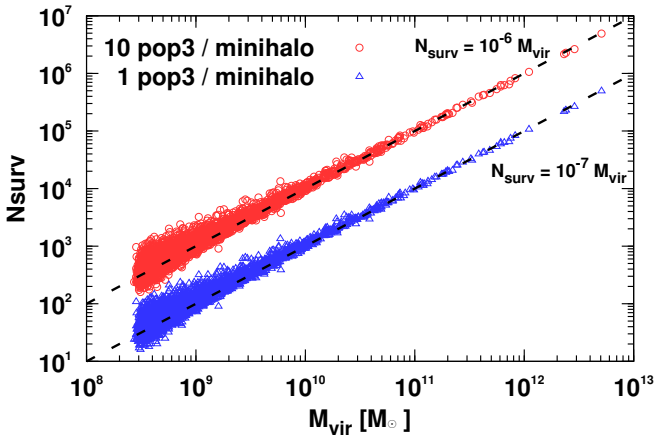

Figure 1. Number of Pop III survivors $N_{\rm surv}$ at $z = 0$ as a function of the halo mass. Blue triangles and red circles show the results of $n_{\rm pop3}$=1 and 10 models. The thick dashed lines show the best-fitting functions (Equation (4) in the text).

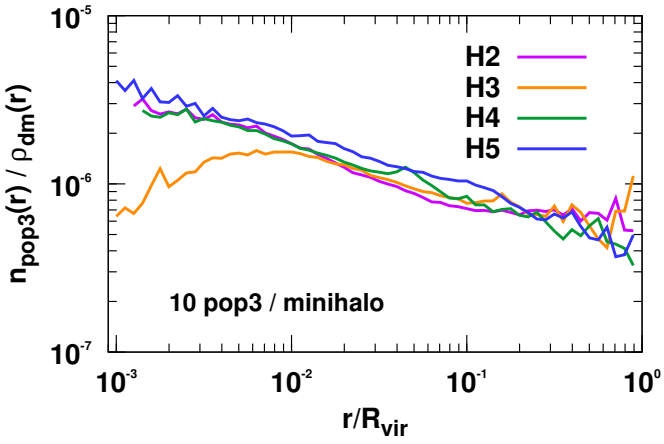

Figure 2. Ratio between radial number density profiles of Pop III survivors $n_{\rm surv}(r)$ and dark matter mass densities of host halos $\rho_{\rm dm}(r)$ for four Milky Way sized halos, H2 to H5. The smallest radii plotted are the reliability limits using criterions suggested by Fukushige & Makino (2001) and Power et al. (2003).

Table 1
The number of particles N, and the virial mass $M_{\rm vir}$ within the virial radius of four Milky Way sized halos in the simulation.

Name	N	$M_{\rm vir}(10^{12}M_\odot)$
H2	381,963,719	2.88
H3	318,640,498	2.40
H4	306,717,590	2.31
H5	146,585,900	1.11

the number of Pop III stars per minihalo, $n_{\rm pop3}$. The best fitting function is given by

$$N_{\rm surv} = 10^{-7} n_{\rm pop3}\frac{M_{\rm vir}}{M_\odot}, \quad (4)$$

where, $M_{\rm vir}$ is the halo virial mass at $z = 0$ with the overdensity according to Bryan & Norman (1998).

This fitting function indicates that the fixed number of survivors, $10^{-7}n_{\rm pop3}$, per one solar dark matter mass

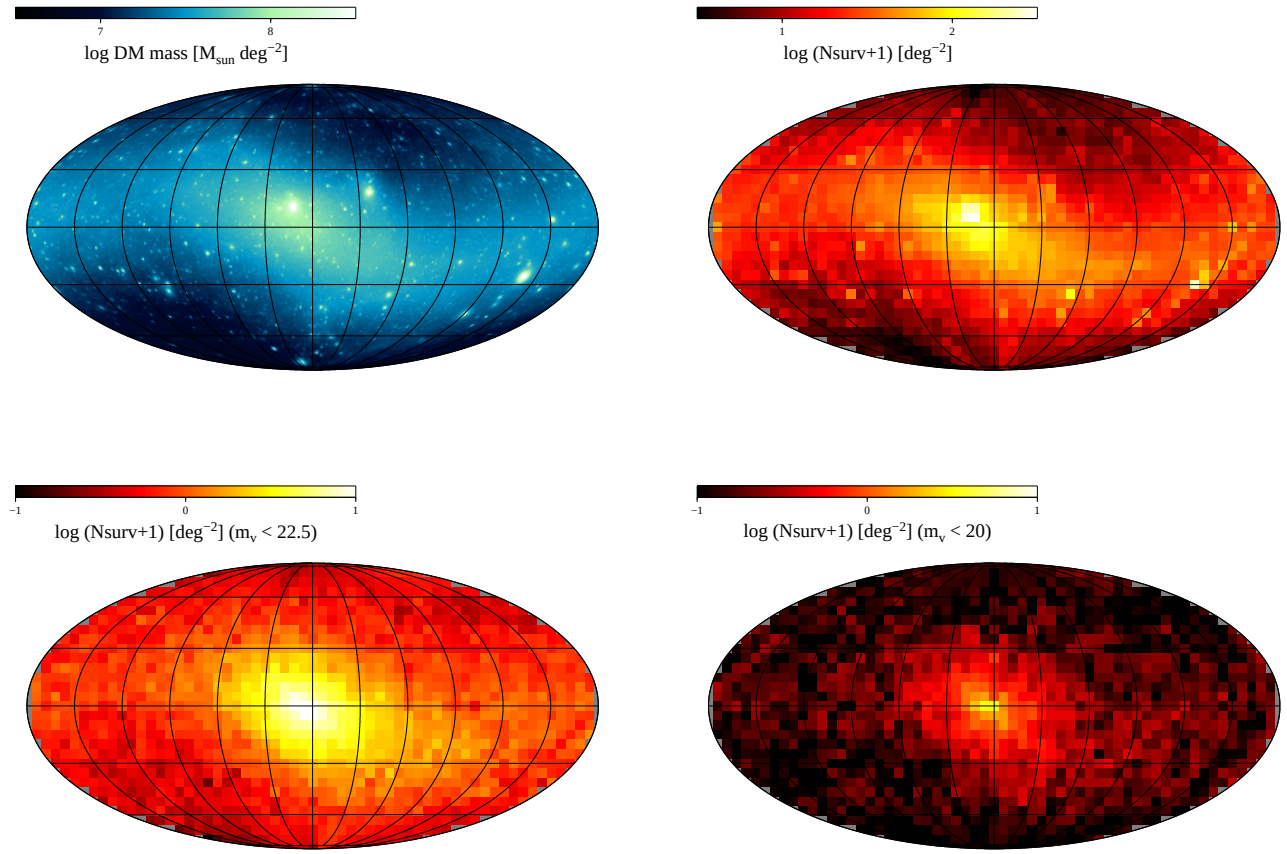

Figure 3. All-sky map of the projected dark matter density and the number density of Pop III survivors in a Milky Way sized halo, H5. The top left panel is the dark matter density. The top right panel shows all survivors. The bottom left and bottom right panels show the number density of survivors with V-band magnitude brighter than 22.5 and 20.0, respectively.

exist in each halo regardless of the halo mass, at least from $\sim 10^8 M_\odot$ to the Milky Way mass. This dependence may be because the dependence of the halo formation history (e.g., merger rate, mass accretion rate) on the halo mass is weak (e.g., Ishiyama et al. 2015).

Hereafter, we focus on the spatial distribution of Pop III survivors in the Milky Way sized halos to discuss their observability, using the $n_{\rm pop3} = 10$ model. In our simulation, four Milky Way sized halos are identified at $z = 0$. In table 1, the number of particles and the virial mass of these halos are summarized. These are second- to fifthmost- massive halos in the entire simulation box. Because the most massive halo (H1: $5.09 \times 10^{12} M_\odot$) is about twice more massive than the Milky Way halo, we exclude this halo in the following analysis.

As described in §2.3, the spatial positions of survivors in these halos are assumed to be those of tracers of dark matter particles directly taken from the high resolution cosmological N-body simulation. This is of great advantage to early studies (e.g., Komiya et al. 2015; Hartwig et al. 2015), based on semi-analytic methods with merger trees extracted from extended Press-Schechter theory (e.g., Press & Schechter 1974; Lacey & Cole 1993). Other early studies based on N-body simulations also suffered from insufficient mass resolution to capture the formation of small minihalos (e.g., Tumlinson 2010).

In Figure 2, we plot the ratio between radial number density profiles of Pop III survivors $n_{\rm surv}(r)$ and dark matter mass densities of host halos $\rho_{\rm dm}(r)$ for four Milky way sized halos, H2 to H5. The survivors tend to be distributed in a manner more concentrated than the dark matter, in particular, in the central regions ($r/R_{\rm vir} < 0.1$), except for H3. This implies that the formation history of H3 might be largely different from the other three halos.

We made the all-sky map of the number density of Pop III survivors in these four halos. The observer is located at 8.5 kpc from the center of the halo. Figure 3 shows all-sky maps of the projected dark matter density and the number density of all survivors per square degree for H5. Clearly, the distribution of survivors reflects that of the dark matter as shown in Figure 2. The survivors tend to be concentrated in the center of the halo and the subhalos.

The distributions of survivors with V-band magnitude brighter than 22.5 and 20.0 are also shown in Figure 3 and are pretty different from that of all survivors. Note that these magnitudes are close to the limiting magnitudes of deep spectroscopic observations like PFS (Takada et al. 2014). The concentrated distribution in subhalos are invisible. This is simply because the subha-

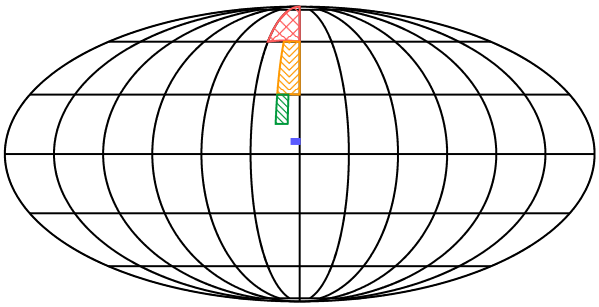

Figure 4. Four target fields in this study are highlighted as gray regions. From top to bottom, these regions correspond to high, middle, low latitude and central fields.

los are too far from the observer. Even if the survivors in the subhalos are bright stars, their apparent magnitude would be faint.

4. OBSERVATION STRATEGY OF Pop III STARS AND CURRENT CONSTRAINTS

While the number of survivors becomes larger toward the center, the stellar components of the Milky Way also show centrally concentrated distribution. Thus, it is not trivial where the observability of survivors is the largest. Previous studies, e.g., Hartwig et al. (2015), had discussed this issue in galactic halo and bulge. However, they had adopted a simple model to distinguish halo and bulge stars because they used a semi-analytic model based on merger trees extracted from extended Press-Schechter theory (e.g., Press & Schechter 1974; Lacey & Cole 1993), which cannot predict the spatial distribution of halos. In contrast to the previous studies, the combination of the cosmological simulation and a Pop III star formation model provides the spatial distribution of survivors in the Milky Way and satellite dwarf galaxies. This enables us to discuss observation strategies to detect Pop III survivors without an additional model.

4.1. *Milky Way*

The Pop III survivors in the Milky Way mix with other stellar components of the Milky Way. Thus, the field stars need to be excluded for the detection of the Pop III survivors. In order to evaluate their detectability in different fields, we extract the stellar distribution and metallicity distribution of the Milky Way using the online interface of the stellar population synthesis model for the Milky Way, Besançon[5] (Robin et al. 2003). The effect of the ISM extinction in the disk was not taken into account.

We calculate the number of survivors and field stars and the sample size required to find one Pop III survivor in the following four different fields:

1. high latitude field : $l = 0°$–$30°$, $b = 60°$–$90°$;
2. middle latitude field : $l = 0°$–$15°$, $b = 30°$–$60°$;
3. low latitude field : $l = 7.5°$–$15°$, $b = 15°$–$30°$; and
4. central field : $l = 0°$–$5°$, $b = 5°$–$7.5°$,

which are displayed in Figure 4. These four fields represent the galactic halo, disk, bulge, and center of the Milky Way. The required sample size is defined as the ratio of the number of field stars to that of survivors. Since most of survivors have a V-band magnitude, $m_{\rm V} > 17$, we do not count field stars brighter than this value.

Figure 5 shows the required sample size in four Milky Way sized halos as a function of V-band limiting magnitude for four different target fields. The result of the $n_{\rm pop3} = 10$ model is shown (solid curves). Dashed curves are the results of this model multiplied by a factor of ten, which mimics the $n_{\rm pop3} = 1$ model. The dependence of the number of survivors on $n_{\rm pop3}$ shown in equation (4) justifies this simple scaling.

In spite of the larger number of survivors toward the galactic center (Figure 3), higher latitude fields require lower sample sizes. This is simply because the field stars are more concentrated at the low latitude field than the survivors. The higher number density of field stars at lower latitude makes the detection of the Pop III survivors less efficient. In the low latitude and central fields, the sample size required is by a factor of $3 \sim 5$ and $30 \sim 200$ larger than those in middle and higher latitude fields, respectively. For all halos, the high latitude field with the direction to the galactic plane ($l = 0°$–$30°$, $b = 60°$–$90°$) are most efficient.

The required sample size is slightly reduced with deep limiting magnitude. This is because the deep observation reaches the stars in the galactic halo. The fraction of survivors in the galactic halo is higher than the galactic disk since the disk star shows more centrally concentrated distribution than that of dark matter. Furthermore, the number of survivors per square degree is increasing as we observe deeper, as indicated in Figure 6, which gives the number density of survivors brighter than the given V-band apparent magnitude per square degree in H5 for four different target fields. However, the weak dependence on the limiting magnitude indicates that a wide and shallow survey detects more survivors than a deep and narrow survey with a given survey power, i.e., telescope and instrument, as long as the number of targets is sufficient.

When we take into account the ISM extinction, the expected number of both survivors and field stars becomes smaller, in particular, for lower latitude fields. We also extract the stellar distribution of the Milky Way with the extinction using the Besançon (Robin et al. 2003) [6]. Figure 7 shows the effect of the ISM extinction on the number of field stars for the central and the low latitude fields, respectively; there is little effect on the low latitude field ($l = 7.5°$–$15°$, $b = 15°$–$30°$). On the other hand, the number of stars at the bright end is largely reduced for the central field ($l = 0°$–$5°$, $b = 5°$–$7.5°$). Assuming that the extinction acts on survivors in the same manner as the field stars, the number density of bright survivors ($m_{\rm V} < 19$) is reduced by a factor of $\sim$2 in only central field.

[5] \protecthttp://model.obs-besancon.fr/

[6] We set the extinction to 0.70 mag/kpc in the galactic disk.

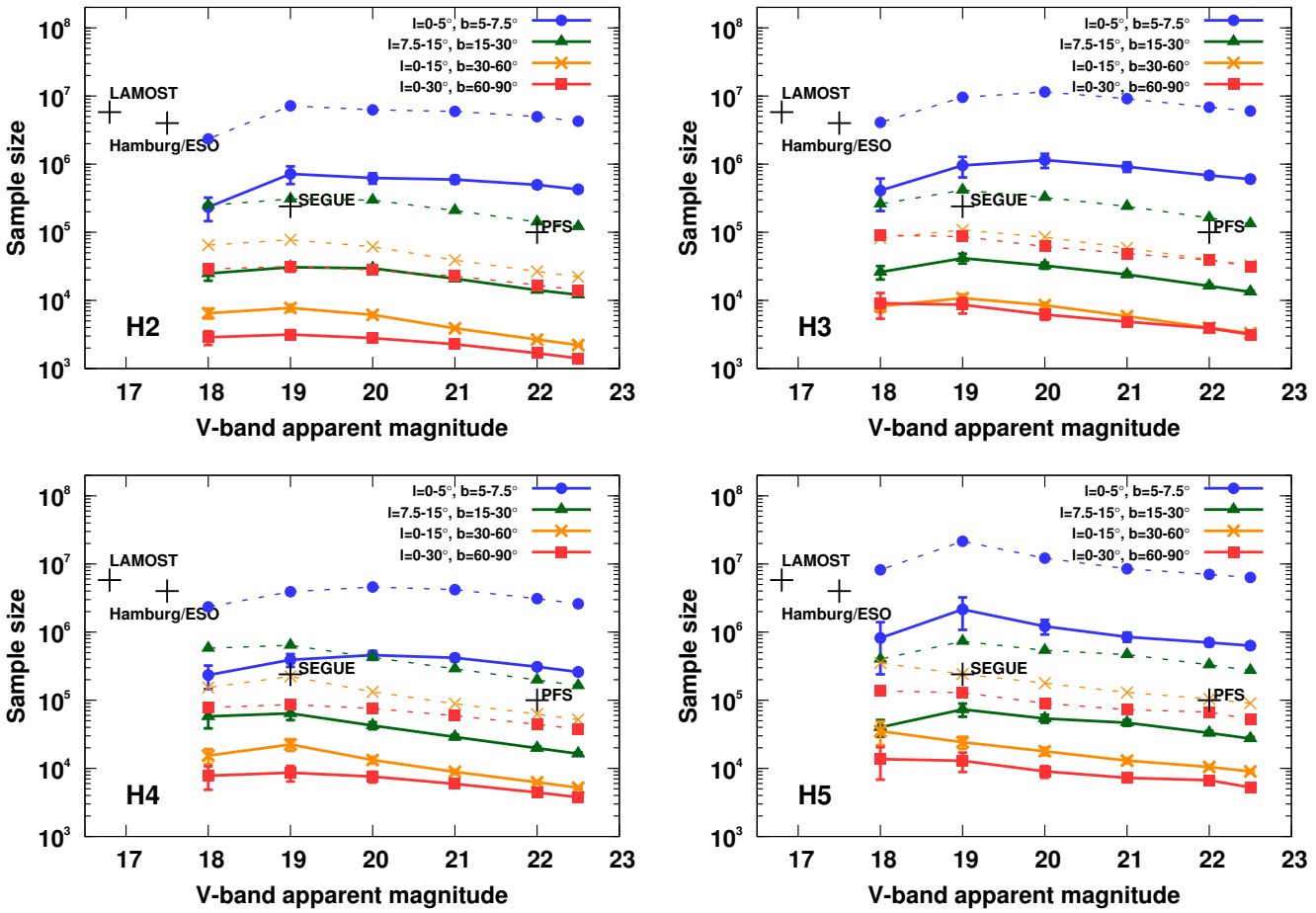

Figure 5. Sample size to find one Pop III survivor in four Milky Way sized halos as a function of V-band magnitude for four different target fields. Solid curves show the results of the $n_{\rm pop3} = 10$ model. Dashed curves are the results of this model multiplied by a factor of ten, which mimics the $n_{\rm pop3} = 1$ model. Crosses show observations, PFS (Takada et al. 2014), SEGUE (Yanny et al. 2009), Hamburg/ESO survey (Christlieb et al. 2008), and LAMOST (Luo et al. 2015), respectively. The error bars show their Poisson error. Since most of survivors have a V-band magnitude, $m_{\rm V} > 17$, we do not count field stars brighter than this value.

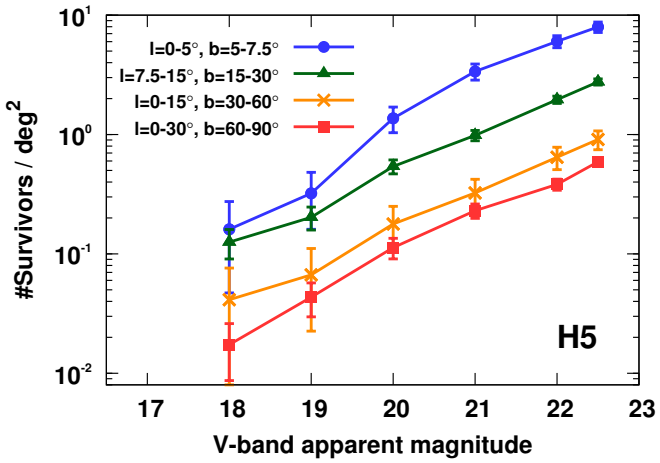

Figure 6. Number density of survivors brighter than the given V-band apparent magnitude per square degree in H5 for four different target fields. The error bars show their Poisson error.

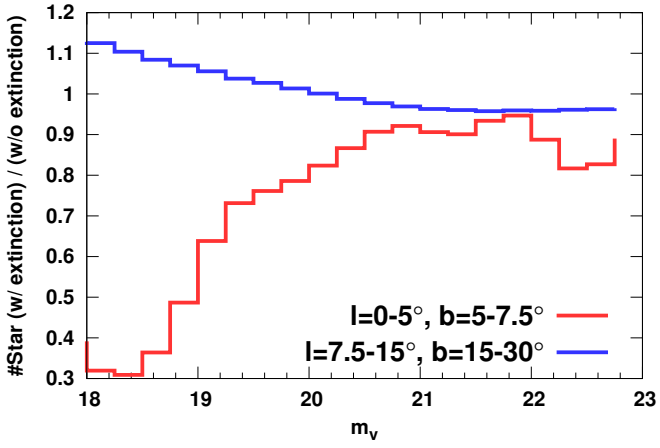

Figure 7. Effect of the ISM extinction on the number of field stars: the ratio between the number with and without the extinction in each V-band magnitude bin.

The observer position does not change the total number of survivors in Milky Way sized halos but can influence those in these fields. To investigate the effect, we calculate the number of survivors seen from randomly placed 1,000 observers on a spherical surface lying 8.5 kpc from the halo center, for high and low latitudes fields of H5, $l = 0°$–$30°$, $b = 60°$–$90°$ and $l = 7.5°$–$15°$, $b = 15°$–$30°$. In table 2, we summarize the median, 5, 25, 75, and 95 percentiles of the sample size for these fields. Regardless of the V-band limiting magnitude m_V,

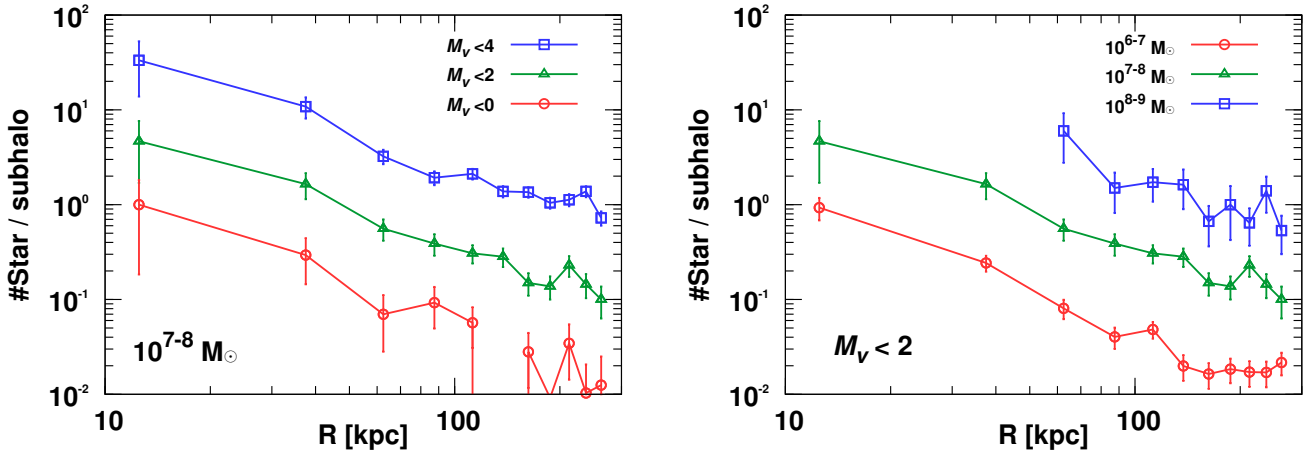

Figure 8. (Left) Radial profile of the average number of Pop III survivors brighter than the given absolute magnitudes in a subhalo of H5 with the mass range of $10^{7-8}M_\odot$ as a function of the radius from the halo center. (Right) Radial profile of the average number of Pop III survivors brighter than absolute magnitudes $M_{\rm V} = 2$ in a subhalo as a function of the radius from the halo center. Three curves correspond to three subhalo mass ranges. The error bars show their Poisson error.

the sample size of the high latitude field (l = 0°–30°, b = 60°–90°) spread by a factor of nearly two and four from 25 to 75 percentiles and from 5 to 95 percentiles. Those of the low latitude field (l = 7.5°–15°, b = 15°–30°) spread by a factor of nearly 1.4 and two from 25 to 75 percentiles and from 5 to 95 percentiles. The 95 percentiles values in the high latitude field are always larger than the 5 percentiles values in the low latitude field.

The spectroscopic metal-poor surveys are mainly conducted at high latitude fields so far. The results of cosmological simulations can be directly compared with outcomes of the past and ongoing/planning surveys. Figure 5 also shows the sample size and limiting magnitude of the following surveys with crosses; Hamburg/ESO survey (Christlieb et al. 2008) , SEGUE (Yanny et al. 2009), and future prospects by PFS (Takada et al. 2014) and LAMOST (Li et al. 2015). If we assume that Hamburg/ESO survey and SEGUE do not detect any survivors and take into account the incompleteness of follow-up moderate dispersion spectroscopy for candidates found by Hamburg/ESO survey (Christlieb 2006), the formation model of Pop III stars with $n_{\rm pop3} = 10$ is already excluded by these observations because the main targets of SEGUE are in relatively higher latitude fields (Figure 1 in Yanny et al. (2009)).

There is a study that suggests that the surface pollution can enhance the surface metal abundance of Pop III survivors up to [Fe/H] ~ -5 (Komiya et al. 2015), below which the Hamburg/ESO survey had found two stars (Christlieb et al. 2002; Frebel et al. 2005). Even if their claim is real, the outcomes of the past surveys still rule out the model with $n_{\rm pop3} = 10$ and favor $n_{\rm pop3} = 1$.

Recently, Skymapper performs a photometric metal-poor survey with a narrow-band filter with a bandpass corresponding to Ca II HK lines and broad-band filters (Keller et al. 2007). Skymapper photometrically excludes the metal-rich field stars and successfully found the most iron-deficient star (Keller et al. 2014) and an extremely metal-poor star in the bulge (Howes et al. 2015). Although the efficiency and completeness of the photometric classification have not been presented, the stars with [Fe/H] > -1.5 is largely excluded (Figure 2 in Howes et al. 2014). Assuming that the photometric classification could exclude 95% of stars with [Fe/H] > -1.5 and adopting the metallicity distribution of the Milky Way model, the numbers of field stars in the high, middle, low latitude, and central fields are reduced by factors of 2.8, 3.8, 7.8, and 17, respectively. The photometric classification enhances the efficiency of follow-up spectroscopy by these factors. As a result, the required sample sizes are comparable in the high and middle latitude fields, while the required sample sizes in the low latitude and central fields are still 2 times and 20 times larger than that of the high latitude field, respectively. Practically, the most efficient field and depth depend on the number of fibers and the field of view of instruments for spectroscopy. If the photometric classification works well, while the high latitude field is most efficient for instruments with low fiber density, e.g., HERMES ($\sim$ 120 fibers/deg^2, Sheinis et al. 2014) for GALAH survey (e.g., De Silva et al. 2015) and LAMOST ($\sim$ 800 fibers/deg^2, Li et al. 2015), the middle latitude field is most efficient for instruments with high fiber density, e.g., PFS ($\sim$ 1800 fibers/deg^2, Takada et al. 2014). By performing spectroscopic observation of a million of stars after the photometric classification in the future, we can constrain the low mass Pop III star IMF with unprecedented accuracy.

4.2. *Dwarf Galaxies*

Only bright survivors are reachable in dwarf galaxies but the distribution of survivors is concentrated (Figure 3). Thus, the detection of survivors in dwarf galaxies could be more efficient than that in the Milky Way. In this subsection, we investigate the possibility of the detection of Pop III survivors in dwarf galaxies. However, the known missing satellite problem (e.g., Klypin et al. 1999; Moore et al. 1999; Ishiyama et al. 2009b) deters the direct prediction from the cosmological simulations and thus we evaluate the average number of Pop III survivors in the model with $n_{\rm pop3} = 10$, brighter than given absolute magnitudes in a subhalo (left panel of Figure 8). The thresholds correspond to absolute magnitudes of the tip of redgiant stars ($M_V = 0$), the redgiant stars ($M_V = 2$), and the turn-off stars ($M_V = 4$). We identify

Table 2
Uncertainty of the sample size by various observational positions. The median, 5, 25, 75, and 95 percentiles of the sample size from 1,000 randomly placed observers are shown. $m_{\rm v}$ is the V-band magnitude cutoff.

Area	$m_{\rm v}$	median	5%	25%	75%	95%
$l = 0$–30°, $b = 60$–90°	22	4.9×10^3	2.3×10^3	3.3×10^3	6.5×10^3	8.8×10^3
$l = 0$–30°, $b = 60$–90°	20	7.8×10^3	4.4×10^3	5.7×10^3	1.1×10^4	1.6×10^4
$l = 7.5$–15°, $b = 15$–30°	22	3.3×10^4	2.2×10^4	2.7×10^4	3.9×10^4	4.8×10^4
$l = 7.5$–15°, $b = 15$–30°	20	6.0×10^4	4.0×10^4	5.1×10^4	7.4×10^4	9.4×10^4

subhalos in each halo with the ROCKSTAR phase space halo/subhalo finder (Behroozi et al. 2013).

While the average number is larger for fainter thresholds, dependence of the average number on the distance from the galactic center is similar. The average number decreases with the distance because the distant subhalos were recently formed and do not satisfy the criteria of Pop III star formation (Sec. 2.2). Furthermore, the average number per subhalo is larger for more massive subhalos (right panel of Figure 8) because the more massive subhalos include more minihalos with Pop III star formation. The inverse of the average number per subhalo is the required number of dwarf galaxies to find one Pop III survivor, if subhalos hosting dwarf galaxies do not preferentially contain a larger number of survivors than all other subhalos. The required number of dwarf galaxies is estimated in less than ten at < 100 kpc for the tip of redgiant stars (corresponding to $m_V \sim 20$), if the dwarf galaxies have a common mass of $\sim 10^7 M_\odot$ (e.g., Strigari et al. 2008; Okamoto & Frenk 2009) although there is a debate (Hayashi & Chiba 2012).

The number of dwarf galaxies discovered so far is nearly 30 (e.g., Koposov et al. 2015; Bechtol et al. 2015). Although the extremely metal-poor stars with [Fe/H] < -3 have been discovered especially in ultra faint dwarf galaxies (e.g., Frebel et al. 2014), no Pop III survivor has been detected. This constraint disfavors $n_{\rm pop3} = 10$ but is consistent with $n_{\rm pop3} = 1$.

Recently, the wide-field photometric surveys newly found dwarf galaxies including ultra faint dwarf galaxies at < 100 kpc (e.g., Belokurov et al. 2007; Laevens et al. 2015). In addition to the large average number of Pop III survivors in nearby dwarf galaxies, the faint threshold can be realized for nearby dwarf galaxies. Thus, the all sky survey of nearby dwarf galaxies is highly demanded for the detection of Pop III survivors. The increasing number of nearby dwarf galaxies refines the constraint on $n_{\rm pop3}$.

In contrast to the Pop III survivors in the Milky Way, the survivors in dwarf galaxies are as faint as $m_V \sim 20$ and the numbers of the detectable Pop III survivors and dwarf galaxies strongly depend on the limiting magnitude. Therefore, the light collecting power is essential on the detection of survivors in dwarf galaxies. Although the number of stars that are bright enough for the high-dispersion spectroscopy with 8m class telescopes is small, candidates of the survivors are reached with the narrow-band imaging and/or low/medium-dispersion spectroscopy with 8-m class telescopes, and will be good targets for the follow-up high-dispersion spectroscopy with 30m class telescopes.

5. DISCUSSION

5.1. *Comparison with Other Studies*

Hartwig et al. (2015) provided the expected number of Pop III survivors in the Milky Way. They reported that an unbiased survey of 4×10^6 halo stars could impose a constraint on the low mass end of the Pop III IMF. This value is more than two orders of magnitude larger than our $n_{\rm pop3} = 10$ model (Figure 5). Even in the $n_{\rm pop3} = 1$ model, more than an order of magnitude difference exists. They used a simple model to distinguish halo and bulge stars because they adopted a semi-analytic model based on merger trees extracted from extended Press-Schechter theory, which could not give the spatial distribution of halos.

In the model of Hartwig et al. (2015), there are physical processes we do not include in our model, dynamical heating of gas during mass accretion and mergers. However, they reported that the main mechanisms to suppress Pop III star formation are metal enrichment at low redshifts and the threshold mass of the minihalo at high redshifts, both of which are included in our model by different manners.

The main reason for such large difference is the adoption of the IMF of Pop IIIstars. Whereas Hartwig et al. (2015) used a logarithmically flat IMF from 0.01 to $100 M_\odot$, we adopted the Kroupa IMF from 0.15 to 1.0 $M_\odot$ for low mass Pop IIIstars. Consequently, the number of low mass Pop III stars per minihalo is also largely different. In their model, the average number was about 0.1 for an IMF in the mass range 0.65 to 100 $M_\odot$ (T. Hartwig 2015, private communication), which is nearly two orders of magnitude smaller than our fixed $n_{\rm pop3} = 10$ model. This large difference is sufficient to explain large gaps in the estimation of the sample sizes needed to constrain on the low mass end of the IMF. From Figure 5, it is easy to infer that the large difference in the estimation of sample sizes would disappear when we used the $n_{\rm pop3} = 0.1$ model, consistent with Hartwig et al. (2015). This means that our and their results qualitatively agree with each other although there is quantitative disagreement.

Why is the average number of Pop III stars per minihalo in both models so different? The decisive difference is that the model of Hartwig et al. (2015) used the lowest mass of the IMF as an arbitrary parameter and tried to constrain it whereas the number of Pop III stars is used in our model. In fact, the lower bound of the IMF $0.65 M_\odot$ in their model was obtained to match the sample size of Hamburg/ESO survey.

The radial number density of survivors (Figure 2) distributes more concentrated than the dark matter and qualitatively agrees with Gao et al. (2010) (see also White & Springel (2000); Diemand et al. (2005); Tumlinson (2010)), although the concentration of our results are less than that of Gao et al. (2010). This quantitative disagreement can be explained by the difference of cosmological parameters. The parameter σ_8 of Gao et al.

(2010) is 0.9, while 0.83 is used in our simulation. The Press-Schechter theory predicts the number of halos of $M \sim 10^6 M_\odot$ at $z = 25$ in $\sigma_8 = 0.9$ by a factor of ~ 3 larger than $\sigma_8 = 0.83$. Because earlier formed progenitor halos tend to concentrate on the center of halos, larger σ_8 should result in a higher concentration of survivors.

One may imagine that the difference can be explained by the way to select tracers of the low mass Pop III stars. Whereas we use randomly selected dark matter particles in minihalos, the most bound particles were used in Gao et al. (2010). Since Pop III stars should be born in the central dense regions of minihalos, they might stay there with a high probability. However, in such situations, Pop III stars could not be long-lived low mass stars because of subsequent mass accretion. On the other hand, some of stars could be kicked away from the central regions of minihalos to regions with shallower potential, via the gravitational many body interaction (e.g., Clark et al. 2011b,a; Smith et al. 2011; Greif et al. 2011a, 2012; Umemura et al. 2012; Susa 2013; Machida & Doi 2013), As a consequence, they could be long-lived low mass stars because of the poor mass accretion, and easily stripped from minihalos by tides of larger halos. Our method to select Pop III tracers mimics this latter process.

To investigate how the distribution of survivors is sensitive to the choice of tracers, we selected the most bound particle from each minihalo as tracers and calculated the radial number density distributions of survivors. Compared with the randomly selected model ($n_{\rm pop3} = 1$), we confirm that both distributions agree well. This suggests that the criteria of Pop III forming minihalos and adopted cosmological parameters are more important for the distributions of survivors, and cosmological radiation hydrodynamical simulations with large volume are necessary to calibrate models.

5.2. *Other Physical Processes*

In this study, we neglect some physical processes that can affect the number of survivors. We will take them into account for our model in future.

Surfaces of Pop III survivors could be polluted with metals (e.g., Yoshii 1981; Shigeyama et al. 2003; Frebel et al. 2009; Komiya et al. 2010, 2015). Frebel et al. (2009) studied the accretion of the ISM on a star in the galactic disk and concluded that it is generally negligible. On the other hand, Komiya et al. (2015) investigated the effect of the ISM accretion in minihalos by a semi-analytic model based on the hierarchical clustering scenario. They demonstrated that the pollution is effective in the early stage of the hierarchical formation of halos and the surface iron abundance of survivors could be enhanced up to [Fe/H] ~ -5. The Fe abundance of hyper metal poor stars (HMP) can be explained by this pollution scenario. Even if we take into account this pollution effect, the models with $n_{\rm pop3} = 10$ are still ruled out because only two stars of [Fe/H]< -5 have been discovered so far. Thus, the main constraint of the Pop III star formation model in our study is not much affected by this effect as discussed in §4.1.

The abundance of the minihalos could be suppressed by the streaming velocities, that is, the supersonic relative velocity of baryon and dark matter arises at the time of recombination (Tseliakhovich & Hirata 2010; Tseliakhovich et al. 2011). Recent numerical simulations including the streaming velocity indicate that typical minihalo mass increases by a factor of three and Pop III star formation is delayed by $\Delta z \sim 4$ (Greif et al. 2011b). On the other hand, Stacy et al. (2011) suggest that there is little effect on the gas evolution by the typical streaming velocity. Currently the effect of the streaming velocity is highly uncertain, and thus, it is needed to evaluate it accurately through large Pop III formation simulations.

5.3. *Remnants of Massive Pop III stars*

In the present paper, we have discussed on the observational possibility of finding Pop III survivors. The effort to search these stars will help to constrain the low mass end of the Pop III IMF at $M \lesssim 1 M_\odot$ severely. On the other hand, the theoretical IMF of Pop III stars extends to $\sim 1000 M_\odot$ (Susa et al. 2014; Hirano et al. 2014, 2015). Thus, it is worth mentioning the observations to be compared with the high mass part of the Pop III IMF.

Metal poor stars could have been born in the remnants of Pop III stars. Hence the comparison of the abundance ratios in the atmospheres of these stars with the theoretical predictions of the nucleosynthesis in the Pop III stars could have great significance in constraining the high mass part of the IMF. In fact, the observed abundance ratios provide little evidence of pair instability supernovae (PISNe), which should be found if some Pop III stars form in the range of $140 M_\odot \lesssim M \lesssim 260 M_\odot$. It is rather consistent with the assumption that most of the Pop III stars are less massive than $100 M_\odot$ to supply the metals by core collapse supernovae (Susa et al. 2014). We have to keep in mind that we cannot directly conclude the less massive ($\lesssim 100 M_\odot$) IMF is favored, because the lack of PISNe pattern is only evident in very metal poor stars with [Fe/H] $\leqq$ -3, and has not been proved for [Fe/H]> -3. In fact, at [Fe/H]$=-2.5$ Aoki et al. (2014) found a possible candidate of a second generation star formed in a remnant of a massive star with $\gtrsim 100 M_\odot$. Further observations of the stars with higher metallicity will give us more information on Pop III IMF. Present high resolution simulations will be coupled with semi-analytical models of low metallicity star formation to be compared with these observations in the near future.

Some theoretical calculations on the Pop III star formation naturally predict formation of multiple stellar systems including massive binaries (Stacy et al. 2012; Susa 2013; Stacy & Bromm 2014; Susa et al. 2014). Such systems will evolve into black hole binaries, which would merge to form a more massive black hole by emitting the gravitational waves. Kinugawa et al. (2016) estimated the detection rate of such events to be pretty high($\sim$180 events yr^{-1}). If the gravitational wave from such objects are detected at a predicted rate, it will be a circumstantial evidence that we are witnessing the merging of Pop III black holes. In fact, the recent discovery of the gravitational wave from $29 M_\odot - 36 M_\odot$ black hole binary coalescence (Abbott et al. 2016) suggests a high rate of such events. The forthcoming data release will provide a better estimate of the frequency. Meanwhile, the high resolution cosmological simulations as presented in this paper will be coupled with Pop III binary formation/evolution theory to give a better prediction of the

event rate from the theoretical side.

6. SUMMARY

If low mass Pop III stars are less massive than $0.8M_\odot$, their lifetime is longer than the cosmic time, and thus they could survive to be found in the Milky Way. We have studied the number and the distribution of low mass Pop III survivors in the Milky Way by combining a large cosmological N-body simulation and a Pop III formation model. Unlike early studies, we can predict the spatial distribution of survivors in the Milky Way by simulating both hierarchical formation of dark matter minihalos and Milky Way halos. We model the Pop III formation in H_2 cooling minihalos without metal under UV radiation of the Lyman-Werner bands. Assuming a Kroupa IMF from 0.15 to 1.0 $M_\odot$ for low mass Pop III as a working hypothesis, we try to constrain the theoretical models in reverse through current and future observations.

From the mass and the collapse redshift of Pop III stars, we calculated the magnitude of various bands using an isochrone model. We selected randomly $n_{\rm pop3}$ dark matter particles from each minihalo as tracers of the low mass Pop III stars. We used $n_{\rm pop3} = 1$ and 10 models. The spatial positions of the tracers at $z = 0$ are assumed to be those of Pop III survivors.

We find that the survivors tend to concentrate on the center of halo and subhalos. We also derived the sample size required to find one Pop III survivor and compare it with past metal-poor star surveys. Since the number density of stars in the galactic disk is too large to negate the increase of the number of survivors toward the galactic center, higher latitude fields require lower sample sizes to detect survivors. If we assume that available observations have not detected any survivors, the formation model of low mass Pop III stars with more than ten stars per minihalo is already excluded.

We also consider practical observation strategies of Pop III survivors in the Milky Way and the dwarf galaxies. The photometric classification with optimized narrow band can largely enhance the efficiency. Provided that the photometric classification could exclude 95% of stars with [Fe/H] > -1.5, the numbers of field stars in the high, middle, low, latitude and central fields are reduced by factors of 2.8, 3.8, 7.8, and 17, respectively. As a result, the required sample sizes are comparable in the high and middle latitude fields, while the required sample sizes in the low latitude and central fields are still 2 times and 20 times larger than that of the high latitude field, respectively.

The required number of dwarf galaxies to find one Pop III survivor is estimated in less than ten at < 100 kpc for the tip of redgiant stars (corresponding to $m_V \sim 20$). Assuming no Pop III survivor has been detected, not $n_{\rm pop3} = 10$ but $n_{\rm pop3} = 1$ is favored, consistent with the current observations of the Milky Way. The all sky survey of nearby dwarf galaxies are highly demanded for the detection of Pop III survivors and refines the constraint on the low mass Pop III IMF.

We also discuss the way to constrain the IMF of Pop III stars at a high mass range of $M \gtrsim 10M_\odot$. For $M < 260M_\odot$, surveys for the metal poor stars at [Fe/H]$\gtrsim -3$ could find the trace of PISNe abundance ratio, if the Pop III IMF extends to the mass range of PISNe as the theories predict.

We thank the anonymous referee for his/her valuable comments. We thank Tilman Hartwig and Wako Aoki for fruitful discussions. Numerical computations were partially carried out on Aterui supercomputer at Center for Computational Astrophysics, CfCA, of National Astronomical Observatory of Japan, and the K computer at the RIKEN Advanced Institute for Computational Science (Proposal numbers hp140212 and hp150226). This work has been funded by MEXT HPCI STRATEGIC PROGRAM. We thank the support by MEXT/JSPS KAKENHI grant No. 15H01030 (TI) and 22540295 (HS).

REFERENCES

Abbott, B. P., Abbott, R., Abbott, T. D., et al. 2016, Physical Review Letters, 116, 061102
Abel, T., Bryan, G. L., & Norman, M. L. 2002, Science, 295, 93
Ahn, K., Iliev, I. T., Shapiro, P. R., et al. 2012, ApJ, 756, L16
Aoki, W., Tominaga, N., Beers, T. C., Honda, S., & Lee, Y. S. 2014, Science, 345, 912
Bechtol, K., Drlica-Wagner, A., Balbinot, E., et al. 2015, ApJ, 807, 50
Beers, T. C., & Christlieb, N. 2005, ARA&A, 43, 531
Behroozi, P. S., Wechsler, R. H., & Wu, H.-Y. 2013, ApJ, 762, 109
Belokurov, V., Zucker, D. B., Evans, N. W., et al. 2007, ApJ, 654, 897
Bromm, V., Coppi, P. S., & Larson, R. B. 2002, ApJ, 564, 23
Bromm, V., & Larson, R. B. 2004, ARA&A, 42, 79
Bryan, G. L., & Norman, M. L. 1998, ApJ, 495, 80
Caffau, E., Bonifacio, P., François, P., et al. 2011, Nature, 477, 67
Christlieb, N. 2006, in Astronomical Society of the Pacific Conference Series, Vol. 353, Stellar Evolution at Low Metallicity: Mass Loss, Explosions, Cosmology, ed. H. J. G. L. M. Lamers, N. Langer, T. Nugis, & K. Annuk, 271
Christlieb, N., Schörck, T., Frebel, A., et al. 2008, A&A, 484, 721
Christlieb, N., Bessell, M. S., Beers, T. C., et al. 2002, Nature, 419, 904
Clark, P. C., Glover, S. C. O., & Klessen, R. S. 2008, ApJ, 672, 757
Clark, P. C., Glover, S. C. O., Klessen, R. S., & Bromm, V. 2011a, ApJ, 727, 110
Clark, P. C., Glover, S. C. O., Smith, R. J., et al. 2011b, Science, 331, 1040
Crocce, M., Pueblas, S., & Scoccimarro, R. 2006, MNRAS, 373, 369
Davis, M., Efstathiou, G., Frenk, C. S., & White, S. D. M. 1985, ApJ, 292, 371
De Silva, G. M., Freeman, K. C., Bland-Hawthorn, J., et al. 2015, MNRAS, 449, 2604
Diemand, J., Madau, P., & Moore, B. 2005, MNRAS, 364, 367
Frebel, A., Johnson, J. L., & Bromm, V. 2009, MNRAS, 392, L50
Frebel, A., Simon, J. D., & Kirby, E. N. 2014, ApJ, 786, 74
Frebel, A., Aoki, W., Christlieb, N., et al. 2005, Nature, 434, 871
Fukushige, T., & Makino, J. 2001, ApJ, 557, 533
Fuller, T. M., & Couchman, H. M. P. 2000, ApJ, 544, 6
Gao, L., Theuns, T., Frenk, C. S., et al. 2010, MNRAS, 403, 1283
Girardi, L., Bressan, A., Bertelli, G., & Chiosi, C. 2000, A&AS, 141, 371
Greif, T. H., Bromm, V., Clark, P. C., et al. 2012, MNRAS, 424, 399
Greif, T. H., Springel, V., White, S. D. M., et al. 2011a, ApJ, 737, 75
Greif, T. H., White, S. D. M., Klessen, R. S., & Springel, V. 2011b, ApJ, 736, 147
Haiman, Z., Thoul, A. A., & Loeb, A. 1996, ApJ, 464, 523
Hartwig, T., Bromm, V., Klessen, R. S., & Glover, S. C. O. 2015, MNRAS, 447, 3892
Hayashi, K., & Chiba, M. 2012, ApJ, 755, 145
Hirano, S., Hosokawa, T., Yoshida, N., Omukai, K., & Yorke, H. W. 2015, MNRAS, 448, 568
Hirano, S., Hosokawa, T., Yoshida, N., et al. 2014, ApJ, 781, 60
Hosokawa, T., Hirano, S., Kuiper, R., et al. 2015, ArXiv e-prints, arXiv:1510.01407

Hosokawa, T., Omukai, K., Yoshida, N., & Yorke, H. W. 2011, Science, 334, 1250
Howes, L. M., Asplund, M., Casey, A. R., et al. 2014, MNRAS, 445, 4241
Howes, L. M., Casey, A. R., Asplund, M., et al. 2015, Nature, 527, 484
Ishiyama, T., Enoki, M., Kobayashi, M. A. R., et al. 2015, PASJ, 67, 61
Ishiyama, T., Fukushige, T., & Makino, J. 2009a, PASJ, 61, 1319
—. 2009b, ApJ, 696, 2115
Ishiyama, T., Nitadori, K., & Makino, J. 2012, in Proc. Int. Conf. High Performance Computing, Networking, Storage and Analysis, SC'12 (Los Alamitos, CA: IEEE Computer Society Press), 5:, (arXiv:1211.4406)
Keller, S. C., Schmidt, B. P., Bessell, M. S., et al. 2007, Publications of the Astronomical Society of Australia, 24, 1
Keller, S. C., Bessell, M. S., Frebel, A., et al. 2014, Nature, 506, 463
Kinugawa, T., Miyamoto, A., Kanda, N., & Nakamura, T. 2016, MNRAS, 456, 1093
Kitayama, T., Susa, H., Umemura, M., & Ikeuchi, S. 2001, MNRAS, 326, 1353
Klypin, A., Kravtsov, A. V., Valenzuela, O., & Prada, F. 1999, ApJ, 522, 82
Komiya, Y., Habe, A., Suda, T., & Fujimoto, M. Y. 2010, ApJ, 717, 542
Komiya, Y., Suda, T., & Fujimoto, M. Y. 2015, ApJ, 808, L47
Koposov, S. E., Belokurov, V., Torrealba, G., & Evans, N. W. 2015, ApJ, 805, 130
Kroupa, P. 2001, MNRAS, 322, 231
Lacey, C., & Cole, S. 1993, MNRAS, 262, 627
Laevens, B. P. M., Martin, N. F., Bernard, E. J., et al. 2015, ApJ, 813, 44
Lewis, A., Challinor, A., & Lasenby, A. 2000, ApJ, 538, 473
Li, H.-N., Zhao, G., Christlieb, N., et al. 2015, ApJ, 798, 110
Luo, A.-L., Zhao, Y.-H., Zhao, G., et al. 2015, ArXiv e-prints, arXiv:1505.01570
Machacek, M. E., Bryan, G. L., & Abel, T. 2001, ApJ, 548, 509
Machida, M. N., & Doi, K. 2013, MNRAS, 435, 3283
Marigo, P., Girardi, L., Chiosi, C., & Wood, P. R. 2001, A&A, 371, 152
Moore, B., Quinn, T., Gvoernato, F., Stadel, J., & Lake, G. 1999, MNRAS, 310, 1147
Nishi, R., & Susa, H. 1999, ApJ, 523, L103
Nitadori, K., Makino, J., & Hut, P. 2006, New A, 12, 169
Okamoto, T., & Frenk, C. S. 2009, MNRAS, 399, L174
Omukai, K., & Nishi, R. 1998, ApJ, 508, 141
Omukai, K., & Palla, F. 2001, ApJ, 561, L55
—. 2003, ApJ, 589, 677
Planck Collaboration, Ade, P. A. R., Aghanim, N., et al. 2014, A&A, 571, A16
Power, C., Navarro, J. F., Jenkins, A., et al. 2003, MNRAS, 338, 14
Press, W. H., & Schechter, P. 1974, ApJ, 187, 425
Robin, A. C., Reylé, C., Derrière, S., & Picaud, S. 2003, A&A, 409, 523
Sakurai, Y., Vorobyov, E. I., Hosokawa, T., et al. 2016, MNRAS, 459, 1137
Scannapieco, E., Kawata, D., Brook, C. B., et al. 2006, ApJ, 653, 285
Sheinis, A., Barden, S., Birchall, M., et al. 2014, in Society of Photo-Optical Instrumentation Engineers (SPIE) Conference Series, Vol. 9147, Society of Photo-Optical Instrumentation Engineers (SPIE) Conference Series, 91470Y
Shigeyama, T., Tsujimoto, T., & Yoshii, Y. 2003, ApJ, 586, L57
Smith, R. J., Glover, S. C. O., Clark, P. C., Greif, T., & Klessen, R. S. 2011, MNRAS, 414, 3633
Stacy, A., & Bromm, V. 2014, ApJ, 785, 73
Stacy, A., Bromm, V., & Loeb, A. 2011, ApJ, 730, L1
Stacy, A., Greif, T. H., & Bromm, V. 2012, MNRAS, 422, 290
Strigari, L. E., Bullock, J. S., Kaplinghat, M., et al. 2008, Nature, 454, 1096
Susa, H. 2013, ApJ, 773, 185
Susa, H., Hasegawa, K., & Tominaga, N. 2014, ApJ, 792, 32
Takada, M., Ellis, R. S., Chiba, M., et al. 2014, PASJ, 66, 1
Tanikawa, A., Yoshikawa, K., Nitadori, K., & Okamoto, T. 2013, New A, 19, 74
Tanikawa, A., Yoshikawa, K., Okamoto, T., & Nitadori, K. 2012, New A, 17, 82
Tegmark, M., Silk, J., Rees, M. J., et al. 1997, ApJ, 474, 1
Tseliakhovich, D., Barkana, R., & Hirata, C. M. 2011, MNRAS, 418, 906
Tseliakhovich, D., & Hirata, C. 2010, Phys. Rev. D, 82, 083520
Tumlinson, J. 2010, ApJ, 708, 1398
Umemura, M., Susa, H., Hasegawa, K., Suwa, T., & Semelin, B. 2012, Progress of Theoretical and Experimental Physics, 2012, 010000
Vorobyov, E. I., & Basu, S. 2015, ApJ, 805, 115
White, S. D. M., & Springel, V. 2000, in The First Stars, ed. A. Weiss, T. G. Abel, & V. Hill, 327
Yanny, B., Rockosi, C., Newberg, H. J., et al. 2009, AJ, 137, 4377
Yoshida, N., Abel, T., Hernquist, L., & Sugiyama, N. 2003, ApJ, 592, 645
Yoshida, N., Omukai, K., & Hernquist, L. 2008, Science, 321, 669
Yoshida, N., Omukai, K., Hernquist, L., & Abel, T. 2006, ApJ, 652, 6
Yoshii, Y. 1981, A&A, 97, 280